Localization and the anomalous Hall effect in a dirty metallic ferromagnet

P. Mitra, N. Kumar, and N. Samarth*
Department of Physics, The Pennsylvania State University, University Park, Pennsylvania 16802, USA
(Received 18 May 2010; revised manuscript received 14 June 2010; published 9 July 2010)

We report magnetoresistance measurements over an extensive temperature range ($0.1 \leq T \leq 100$ K) in a disordered ferromagnetic semiconductor ($Ga_{1-x}Mn_xAs$). The study focuses on a series of metallic $Ga_{1-x}Mn_xAs$ epilayers that lie in the vicinity of the metal-insulator transition ($k_F l_e \sim 1$). At low temperatures ($T < 4$ K), we first confirm the results of earlier studies that the longitudinal conductivity shows a $T^{1/3}$ dependence, consistent with quantum corrections from carrier localization in a "dirty" metal. In addition, we find that the anomalous Hall conductivity exhibits universal behavior in this temperature range with no pronounced quantum corrections. We argue that the observed scaling relationship between the low-temperature longitudinal and transverse resistivity, taken in conjunction with the absence of quantum corrections to the anomalous Hall conductivity, is consistent with the side-jump mechanism for the anomalous Hall effect. In contrast, at high temperatures ($T \gtrsim 4$ K), neither the longitudinal nor the anomalous Hall conductivity exhibit universal behavior, indicating the dominance of inelastic-scattering contributions down to liquid-helium temperatures.

DOI: 10.1103/PhysRevB.82.035205 PACS number(s): 75.47.−m, 72.15.Rn, 75.50.Pp, 81.05.Ea

I. INTRODUCTION

The anomalous Hall effect (AHE) refers to an excess transverse Hall voltage arising from the influence of spin-orbit coupling on the motion of charge carriers in a spin-polarized metal. The phenomenon first attracted attention several decades ago[1–4] and still continues as an active area for theoretical[5–10] and experimental[10–15] inquiry. Calculations have identified two classes of underlying mechanisms for the AHE: "extrinsic" contributions originating from the spin-dependent scattering of carriers by impurities[2,4] and "intrinsic" ones that involve the interaction of carrier spins with the inherent crystal band structure.[1,16] A number of experiments have aimed to identify the mechanisms responsible for the AHE in different materials (see Ref. 10 for a complete bibliography). This is commonly addressed by examining a scaling relationship of the form $\rho_{xy} \sim \rho_{xx}^{\alpha}$, where ρ_{xx} and ρ_{xy} are the longitudinal and transverse resistivity, respectively. Theory predicts $\alpha = 2$ for the intrinsic mechanism.[1] In the extrinsic case, the exponent depends on the nature of the spin-dependent scattering mechanism: $\alpha = 1$ for skew scattering[2] and $\alpha = 2$ for the side-jump mechanism.[4]

Three regimes emerge from these experimental studies:[10] (1) at low disorder, the scaling exponent $\alpha = 1$, suggesting that the AHE is dominated by skew scattering; (2) at moderate disorder, $\alpha = 2$, resulting in a Hall conductivity σ_{xy} which is independent of disorder (since $\sigma_{xy} = \frac{\rho_{xy}}{\rho_{xx}^2}$). This scaling is consistent with both the intrinsic mechanism and the extrinsic side-jump mechanism but it is difficult to convincingly distinguish between these using dc transport; and (3) at large disorder, numerical calculations report $\alpha \approx 1.6$. While there is no simple physical explanation for this behavior, this scaling does appear to emerge from numerical calculations of the anomalous conductivity in the hopping regime.[7]

A cautionary note arises in the interpretation of such experimental data: the analysis of the scaling relationship should strictly be carried out at temperatures where impurity scattering dominates and other inelastic processes (such as scattering from spin waves) have been frozen out. In this paper, we describe measurements of the AHE in a canonical ferromagnetic semiconductor ($Ga_{1-x}Mn_xAs$) over a large temperature range (100 mK $\leq T \leq$ 150 K). Our study is restricted to samples whose resistivity lies in a regime $2 \lesssim \rho_{xx} \lesssim 10$ mΩ cm where other studies[11,13] have observed an AHE scaling exponent $\alpha = 2$ at $T \geq 4.2$ K. These observations have been interpreted as an insensitivity to disorder and thus as a signature of the intrinsic mechanism,[11] in agreement with theoretical predictions made in the disorder-free limit.[9] However, we argue that unlike metallic ferromagnets where the Drude approximation works well at helium temperatures, the complex nonmonotonic temperature dependence of the resistivity in $Ga_{1-x}Mn_xAs$ provides strong motivation for systematic measurements at lower (dilution fridge) temperatures where impurity scattering is dominant. Our principal aim is to test the robustness of the scaling relationship by examining it at such lower temperatures. Our study also allows us to address another interesting question that has thus far been ignored in $Ga_{1-x}Mn_xAs$: what (if any) are the quantum corrections to the anomalous Hall conductivity? This question is particularly germane within the context of $Ga_{1-x}Mn_xAs$, where the confluence of ferromagnetism disorder and interactions invariably occurs in close vicinity of the metal-insulator transition (MIT) (Ref. 17). Earlier studies[6,18] on metallic ferromagnets in the weak-disorder limit ($k_F l_e \gg 1$, where k_F and l_e are the Fermi wave vector and the elastic mean-free path, respectively) show that the quantum correction to the anomalous Hall conductivity is distinctly different for the skew-scattering and side-jump mechanisms, thus providing an alternative route to test the origin of the AHE. We are however unaware of any theoretical calculations addressing the corresponding quantum correction for the intrinsic mechanism.

II. EXPERIMENTAL DETAILS

Our measurements center on a set of five $Ga_{1-x}Mn_xAs$ samples grown by low-temperature molecular-beam epitaxy with Mn composition in the range $0.028 \leq x \leq 0.078$. The

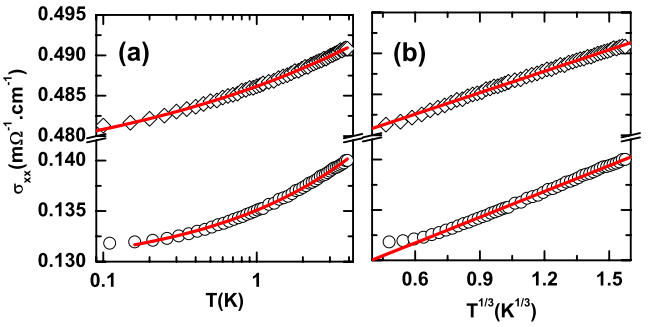

FIG. 1. (Color online) (a) Plot of conductivity vs temperature on a log scale for as-grown $x=0.03$ (diamonds) and annealed $x=0.08$ (circles) $Ga_{1-x}Mn_xAs$. Solid lines represent fits to $\sigma_{xx}(T)=\sigma_{xx}^0+AT^n$. (b) Plot of conductivity of the same samples vs $T^{1/3}$. Solid lines are linear fits.

samples are all 120 nm thick with the exception of the sample with $x=0.078$ which is 50 nm thick. A detailed description of the growth and characterization of these samples has been provided earlier.[19,20] In order to generate a larger phase space of conductivity, we measure both as-grown and annealed pieces of these samples. The annealing is known to simultaneously increase the hole density and decrease the disorder by reducing the density of hole-compensating Mn interstitial defects.[19,20] Transport measurements are carried out on lithographically defined Hall bars (400×100 μm^2) in a Quantum Design dilution refrigerator with the sample temperature ranging from 100 mK to 4 K. (Although the nominal base temperature of the dilution fridge is 50 mK, we find that samples do not cool down efficiently below 100 mK and thus exclude the corresponding data from our analysis.) We measure longitudinal and transverse resistances simultaneously using a standard double lock-in technique with an ac excitation of 100 nA (optimal for measuring the small Hall signal while minimizing sample heating). To avoid contributions to the small Hall voltage from the significantly larger longitudinal voltage, we carry out measurements at positive and negative applied magnetic field $B=0.5$ T (sufficient to fully polarize magnetic domains) and use the standard antisymmetrization procedure. We note that—due to the large hole density ($p\geq10^{20}$ cm^{-3})—the contribution of the ordinary Hall effect is negligible compared to the AHE. Since our analysis relies on knowledge of the hole carrier density, we also note that the values used here are determined using Raman measurements,[21] reducing the uncertainties that are typically involved in deducing the carrier density in the presence of the AHE.

III. QUANTUM CORRECTIONS TO THE LONGITUDINAL CONDUCTIVITY

We first address the temperature dependence of the zero-field conductivity ($\sigma_{xx}=1/\rho_{xx}$) shown in Fig. 1(a) for two extremes in our sample set: the as-grown sample with $x=0.028$ has the lowest value of σ_{xx} while the annealed sample with $x=0.078$ has the highest σ_{xx}. An unbiased fit of the data to the functional form: $\sigma_{xx}(T)=\sigma_o+AT^n$ with the exponent n as a free-fitting parameter, yields $0.2\lesssim n\lesssim0.4$ for different samples. Based on the known functional forms for the temperature dependence of σ_{xx} in three dimensional (3D) disordered systems, combined with earlier analyses of $Ga_{1-x}Mn_xAs$ (Ref. 22), $In_{1-x}Mn_xAs$, (Ref. 23), and (nonmagnetic) n-GaAs (Ref. 24), we conclude that our data is most appropriately described by $n=1/3$. Indeed, a plot of σ_{xx} vs $T^{1/3}$ shows a linear dependence over almost two decades of variation in T [Fig. 1(b)]. As we discuss below, the $T^{1/3}$ dependence of conductivity in 3D disordered systems has been predicted within the context of the scaling theory of localization in the "dirty-metal" regime.[25] We note that other studies of the temperature-dependent conductivity in $Ga_{1-x}Mn_xAs$ have taken a different interpretation, assigning a $\sigma_{xx}\sim T^{1/2}$ dependence which arises from electron-electron interactions.[26] However, forcing a $T^{1/2}$ fit to our data yields a systematic variation in the residual plot, leading us to discount this dependence as providing a physically meaningful description of the data. We also note that the $\sim T^{1/2}$ dependence is derived from perturbative calculations that apply only to weakly disordered systems ($k_Fl_e\gg1$) while even the best $Ga_{1-x}Mn_xAs$ samples fabricated to date are highly disordered and always close to the MIT. For the samples studied here, we estimate Drude values of $l_e\sim0.5-1.3$ nm and $k_Fl_e\sim1-2$ using the extrapolated zero-temperature values of σ_{xx}.

As first pointed out by Altshuler and Aronov,[25] in the vicinity of the MIT, the disorder-dependent correlation length is larger than relevant temperature-dependent length scales, resulting in a temperature variation in the scale dependence of the diffusion constant D (Ref. 27). This contrasts with the weak-disorder regime where D is independent of temperature. One possibility is that the dominant temperature-dependent length scale is the interaction length defined as $L_T=\sqrt{\hbar D/k_BT}$: physically, this characterizes the length over which coherence is maintained during the elastic scattering of quasiparticles that lie within k_BT of the Fermi energy. In this case,[28] the prefactor of $T^{1/3}$ is proportional to the density of states N; specifically, $A=(e^2/\hbar)(G_c^2Nk_B)^{1/3}$, where G_c is the critical conductance and k_B is the Boltzmann constant. Another possibility is that the dominant length scale is the inelastic length $l_{in}=\sqrt{D\tau_\phi}$ which characterizes the diffusive motion of electrons between inelastic collisions.[29] Here, the dephasing rate is $\tau_\phi^{-1}=aT$ and the prefactor of $T^{1/3}$ is $A=(e^2/\hbar)(G_cNak_B)^{1/3}$. A relevant dephasing mechanism in dirty metals is that due to the electron-electron interaction;[30] in this case, $a\sim(k_Fl_e)^{-2}$. Hence, the prefactor A should depend on both disorder and carrier density. We note that in $Ga_{1-x}Mn_xAs$ other possible dephasing mechanisms may also exist, including scattering from spin waves or from two-level systems formed at Mn interstitial sites.[31] However, we do not anticipate an explicit dependence on disorder in the latter cases.

Figure 2(a) plots the prefactor A as a function of the Mn concentration (x) for both as-grown and annealed samples, revealing a nonmonotonic dependence wherein A reaches a minimum at $x\sim0.056$. Since Mn acts both as an acceptor that generates holes and also adds to the disorder in the form of interstitials, we speculate that—for given growth conditions—there exists an optimal Mn-doping level that maximizes the carrier density and minimizes disorder.

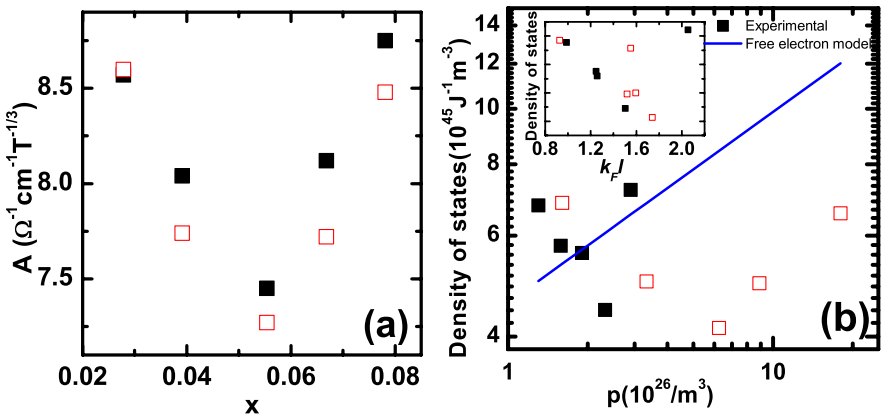

FIG. 2. (Color online) (a) Prefactor A vs Mn concentration obtained from numerical fits of the conductivity data to $\sigma_{xx}(T)=\sigma_{xx}^{0}+AT^{1/3}$. (b) Experimental estimate of the density of states $(\hbar A/e^2)^3/k_B$ vs hole density. The solid line shows the expected value for a free-electron gas. Inset shows the density of states versus $k_F l_e$. The filled and open squares represent as-grown and annealed samples, respectively.

Further—for a given Mn concentration—A is found to decrease upon annealing which is known to increase the hole carrier density. This is inconsistent with the interaction picture that predicts A to increase if p increases. Thus, the data in Fig. 2(a) indirectly suggest that A varies with disorder and that the $T^{1/3}$ dependence is possibly due to localization rather than interactions.

Recent experiments on mesoscopic $Ga_{1-x}Mn_xAs$ samples[32,33] estimate inelastic path lengths $l_{in}\sim 100$ nm for $x=0.02$ at 10 mK and for $x=0.06$ at 100 mK, respectively, and a dephasing time τ_ϕ that varies inversely with temperature at higher temperatures ($T\lesssim 1$ K). This places our samples of thickness $t=120$ nm in the 3D regime (wherein the film thickness exceeds the inelastic length l_{in}) in the temperature range of interest (100 mK$\leq T\leq$4 K). Further, if we compare these estimates for the inelastic path lengths with our Drude estimates of the elastic path length, we find that the condition $l_{in}>l_e$ is indeed satisfied in our samples. Figure 2(b) plots the quantity $N=(\hbar A/e^2)^3/G_c^2 k_B$, as a function of p and $k_F l_e$ (inset), where we use $G_c=3\pi^3/2$ (Ref. 28). Note that in the interaction picture,[28] N is indeed the density of states while in the localization case,[29] N depends on both density of states and disorder. As shown in Fig. 2, N does not follow any systematic dependence on p and decreases with increasing $k_F l_e$ (inset), again supporting the localization picture (the $t=50$ nm samples do not follow the trend).

IV. ABSENCE OF QUANTUM CORRECTIONS TO THE ANOMALOUS HALL CONDUCTIVITY

We now address the quantum corrections to σ_{xy} by using the temperature variation in ρ_{xx} and ρ_{xy}. We find that for all our samples, both ρ_{xx} and ρ_{xy} increase monotonically with decreasing temperature in the range 100 mK$\leq T\leq$4 K and we observe that the temperature dependence can be fit to the functional form $\rho_{ij}(T)=\rho_{ij}^{0}+A_j T^{1/3}$. Thus at $T=0$ K, the resistivity extrapolates to a finite ρ_{ij}^{0} and is found to be positive for both longitudinal and Hall components for each sample. To estimate the magnitude of the quantum corrections, we examine the relative changes of the resistivity with respect to the zero-temperature value $\delta_T\rho_{ij}=[\rho_{ij}(T)-\rho_{ij}(0)]/\rho_{ij}(0)$. We also examine the relative change in the anomalous Hall conductivity calculated using $\sigma_{xy}=\rho_{xy}/(\rho_{xx}^2+\rho_{xy}^2)$. Figures 3(a) and 3(b) plot $\delta_T\rho_{xx}$, $\delta_T\rho_{xy}$, and $\delta_T\sigma_{xy}$ as a function of $T^{1/3}$. Linear fits to the data indicate that the slope $\delta_T\rho_{xy}$ is double that of $\delta_T\rho_{xx}$. Also, $\delta_T\sigma_{xy}$ does not show any pronounced temperature dependence and is scattered around zero over the temperature range. Using the approximation $\sigma_{xy}\approx\rho_{xy}/\rho_{xx}^2$, it is easy to show that the following identity summarizes the universal scaling behavior observed in all our samples

$$\delta_T\rho_{xy}=2\delta_T\rho_{xx}\Rightarrow\delta_T\sigma_{xy}=0. \quad (1)$$

Thus, we report a key experimental finding: there are no quantum corrections to σ_{xy}^{AH} in metallic $Ga_{1-x}Mn_xAs$ over the temperature range of 100 mK$\leq T\leq$4 K where σ_{xx} exhibits a finite-localization correction in the form of $T^{1/3}$. We are not aware of any theoretical calculations that support our findings in this high-disorder regime. However, we note that calculations of quantum corrections to the anomalous Hall conductivity in *weakly disordered* ferromagnets[6,8] do indeed show that—in contrast to the skew-scattering mechanism—the side-jump mechanism results in a negligible temperature dependence of σ_{xy}. Speculating that the essential nature of this low-disorder result is unchanged at high disorder, our observations could be consistent with the side-jump mechanism.

V. BEHAVIOR OF LONGITUDINAL AND ANOMALOUS HALL CONDUCTIVITY AT HIGH TEMPERATURES

To further corroborate the uniqueness of the low-temperature results described above, we carried out measurements on our samples at higher temperatures ($T\geq 4.2$ K), up to the Curie temperature T_C of the samples. Not surprisingly, we find that the universal scaling of ρ_{xx} and ρ_{xy} (which leads to a constant σ_{xy} at low temperatures) breaks down at higher temperatures. As is well known, the temperature dependence of ρ_{xx} shows a peak near T_C and decreases to a minimum

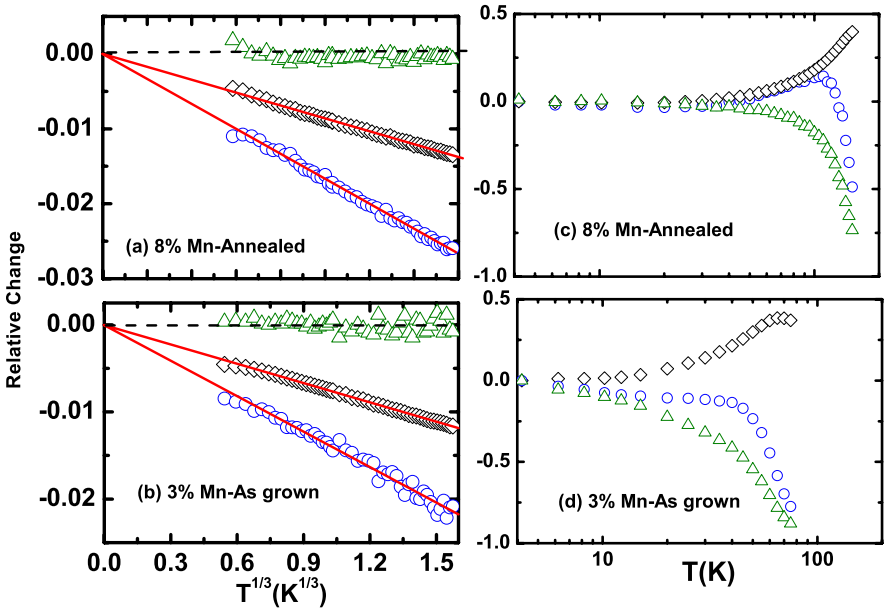

FIG. 3. (Color online) Relative changes in the longitudinal resistivity (diamonds), the anomalous Hall resistivity (circles), and the anomalous Hall conductivity (triangles) for two $Ga_{1-x}Mn_xAs$ samples. In (a) and (b), these are plotted as a function of $T^{1/3}$ for $0.1 \leq T \leq 4$ K. Solid lines are linear fits to the data. In (c) and (d), these quantities are plotted vs T for $T \geq 4$ K.

around $T \sim 8-15$ K, showing a much weaker monotonic increase with decreasing temperature. The temperature dependence of ρ_{xx} for $T \geq 4$ K has recently been interpreted within a scaling-analysis picture that takes into account the competition between localization and the onset of magnetic ordering.[34] However, the temperature dependence of ρ_{xy} and σ_{xy} has not been studied previously in great detail over a wide range of samples. We find a nonuniversal behavior in the relative scaling of ρ_{xx} and ρ_{xy} at high temperature. Figures 3(c) and 3(d) plot the temperature dependence of the relative changes in ρ_{xx}, ρ_{xy}, and σ_{xy} with respect to their values at $T=4.2$ K. For low Mn content samples, ρ_{xy} decreases monotonically with increasing temperature in the regime 4.2 K $\leq T \leq T_C$, as shown in Fig. 3(d). For higher Mn content samples, the temperature variation in ρ_{xy} is nonmonotonic over this temperature range. As shown in Fig. 3(c), the relative changes in ρ_{xy} and ρ_{xx} increase with the same rate up to $T \sim 90$ K; at even higher temperatures, ρ_{xy} decreases rapidly as T_C is approached. In both cases, magnetometry measurements (data not shown) show that the saturated magnetization M_s decreases monotonically as T increases. The observations are consistent with the view that in low T_C ferromagnets such as $Ga_{1-x}Mn_xAs$, magnetic fluctuations play an important role at high temperatures ($T \gtrsim 8$ K) and dominate the temperature dependence of the resistivity.[34] In such regimes, scattering from magnetic impurities may contribute to the AHE with ρ_{xy} proportional to magnetic fluctuations of the form $\langle (M - \langle M \rangle)^3 \rangle$. We speculate that this "Kondo-type" AHE may be more relevant at high temperatures.

In this high-temperature regime, σ_{xy} decreases monotonically for $T \geq 4.2$ K, as shown in Figs. 3(c) and 3(d). The temperature dependence of σ_{xx} and σ_{xy} clearly demarcates two regimes: at low temperature ($T \lesssim 4.2$ K), we find a universal behavior for the entire sample set arising from localization corrections while at higher temperatures ($T \gtrsim 4.2$ K), the behavior is completely different and nonuniversal. Based on the above result, we argue that analyses of the AHE scaling relationship in $Ga_{1-x}Mn_xAs$ are only meaningful if they are carried out in the former low-temperature regime. For instance, we obtain identical and consistent results if we carry out the scaling analysis using either the extrapolated zero-temperature resistivities (obtained from the $T^{1/3}$ dependence of ρ_{xx} and ρ_{xy}) or using the resistivity value measured at the base temperature of our dilution refrigerator (<100 mK) which is a stable, reproducible lowest temperature achievable. In both cases, the following results are found to be the same. However, scaling carried out at higher temperatures produces significant departures.

VI. SCALING ANALYSIS OF THE ANOMALOUS HALL EFFECT AT LOW TEMPERATURES

We now discuss the scaling of our AHE data at low temperature. We begin with the standard scaling relation of the anomalous Hall resistivity normalized by the saturated magnetization M_s (anomalous Hall coefficient) $R_s = \rho_{xy}/M_s$ [Fig. 4(a)]. A log-log plot of R_s vs ρ_{xx} shows a linear dependence indicative of a power-law behavior of the form $R_s \sim \rho_{xx}^{\alpha}$. Linear fits to the data yield an exponent of $\alpha = 2.07 \pm 0.09$. This implies that within experimental error $R_s/(\rho_{xx}^o)^2 = \sigma_{xy}^o/M_s$ is independent of the variation in the hole carrier density p and disorder in the sample set under consideration. However, unlike metallic systems where the above result can perhaps be directly interpreted as a manifestation of the side-jump mechanism, the situation in $Ga_{1-x}Mn_xAs$ is more complex and requires further examination. This is because the variation in Mn composition between different samples and the annealing of a given sample results in a simultaneous varia-

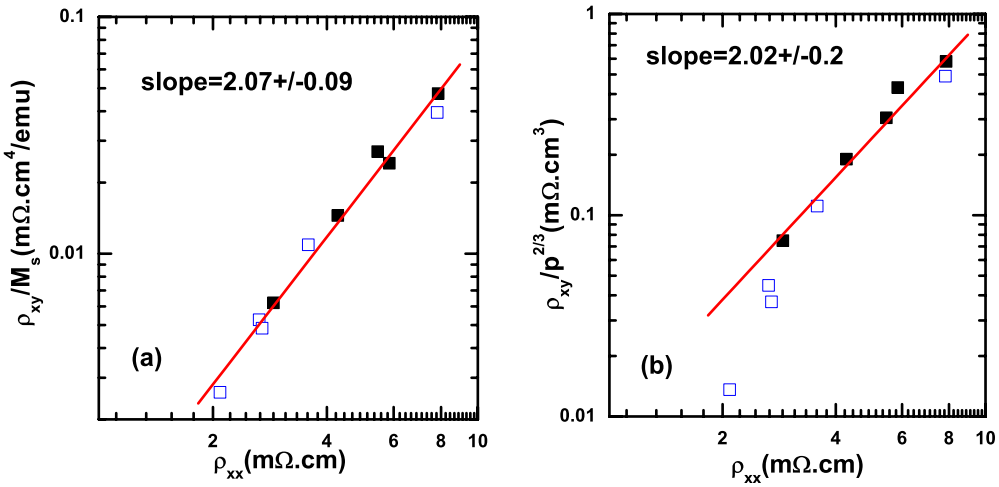

FIG. 4. (Color online) (a) Zero-temperature AH resistivity normalized by magnetization vs the zero-temperature longitudinal resistivity and (b) Zero-temperature AH resistivity normalized by magnetization vs $p^{2/3}$. Linear fits to these log-log plots indicate power-law dependence with exponents given by the slopes. Closed (open) symbols represent as-grown (annealed) samples.

tion in the magnetization, the hole carrier density and the point defect density.

In ferromagnetic metals, the magnetization arises directly from the spin imbalance in the conduction band while the AH voltage arises from spin-dependent scattering and is directly proportional to the magnetization. In contrast, $Ga_{1-x}Mn_xAs$ is not a band ferromagnet and the magnetization is due to the ferromagnetically coupled localized moments on the substitutional Mn atoms. However, the valence band in $Ga_{1-x}Mn_xAs$ has a high degree (~90%) of spin polarization.[35,36] Consequently, if we assume that the net spin imbalance is proportional to the exchange field experienced by the carriers and hence the magnetization ($p_\uparrow - p_\downarrow \propto M_s$), we encounter a situation similar to a metal as far as the AHE is concerned. Thus, the result shown in Fig. 4(a) can indeed be interpreted as a manifestation of the side-jump mechanism. We estimate the AH conductivity for the side-jump mechanism using the simplified expression for a fully spin-polarized single-band system: $\sigma_{xy}=(e^2/\hbar)(p\Delta_{SJ}/k_F)$ (Ref. 4). Using typical values for the carrier density of $Ga_{1-x}Mn_xAs$ in the range of $10^{20}-10^{21}/cm^3$, we estimate $\sigma_{xy}^{SJ} \sim 13-63\ \Omega^{-1}\,cm^{-1}$ (using $\Delta_{SJ}=0.1$ nm) which is of same order of magnitude as our experimental values of $10-22\ \Omega^{-1}\,cm^{-1}$.

To further explore the picture of the side-jump mechanism assuming full spin polarization of carriers, we examine the scaling behavior of the AH resistivity. If the side-jump mechanism indeed contributes to the AH conductivity through the expression given earlier, then we expect that $\rho_{xy}^o/p^{2/3} \propto (\rho_{xx}^o)^2$ (Ref. 2) [assuming for simplicity a free-electron dependence $k_F=(3\pi^2 p)^{1/3}$]. Figure 4(b) shows a plot testing this scaling: excluding the three lowest resistivity samples, a linear fit to the data yields an exponent of $\alpha \sim 2.02 \pm 0.2$, implying both that σ_{xy} is independent of disorder and that the data are consistent with the side-jump mechanism. The fact that the high p samples deviate downwards from the linear dependence is due to the overestimation of the net spin imbalance in the single-band approximation: strictly speaking, the analysis in Fig. 4(b) should be carried out with the net carrier spin imbalance ($p_\uparrow - p_\downarrow$) rather than the total carrier density p. From the fitting parameters, we estimate the side-jump length to be (0.07 ± 0.04) nm.

Much interest has been generated by the theoretical prediction[9] of "dissipationless" anomalous Hall current in $Ga_{1-x}Mn_xAs$, originating from purely band structure effects even in the absence of impurity scattering. Calculations in the disorder-free case successfully predict the qualitative features of the AHE (the sign and rough magnitude of σ_{xy}) in different III-V diluted magnetic semiconductors. As mentioned earlier, recent experiments[11,13] carried out at high temperatures ($T \sim 10-15$ K) have been interpreted using this picture of an intrinsic AHE in $Ga_{1-x}Mn_xAs$, albeit with the idealized assumption that compensation is absent. In our sample set, we estimate p to be in the range of 10–60 % of the total Mn-dopant concentration, indicating a high degree of compensation due to the presence of interstitials. The only exception was the annealed sample of $x=0.078$ with a thickness of 50 nm that is found to be close to the limit of no compensation. Thus, our data cannot provide a rigorous test of the validity of the intrinsic-mechanism scenario.

VII. CONCLUSIONS

To conclude, we have carried out a systematic study of the temperature-dependent longitudinal and anomalous Hall conductivity in a ferromagnetic semiconductor close to the the metal-insulator transition. We find that carrier localization rather than interaction effects provide the dominant quantum correction to σ_{xx} while our data show no quantum corrections to σ_{xy}. Further, we find that the absence of temperature dependence in σ_{xy} and the scaling relationship between ρ_{xy} and ρ_{xx} is consistent with the side-jump mechanism for the AHE. However, a more rigorous interpretation of these experimental observations will require more detailed calculations for the AHE in $Ga_{1-x}Mn_xAs$ that explicitly take into account the high degree of disorder in the samples.

ACKNOWLEDGMENTS

We thank S. Potashnik, K. C. Ku, and S. H. Chun for sample growth. The authors thank the Penn State Center for Nanoscale Science (funded by NSF under Grant No. DMR-0820404) for the use of low-temperature measurement facilities. This work was also partially supported by NSF under Grant No. DMR-0801406.

*nsamarth@phys.psu.edu

[1] R. Karplus and J. M. Luttinger, Phys. Rev. **95**, 1154 (1954).
[2] J. Smit, Physica (Amsterdam) **21**, 877 (1955).
[3] J. Kondo, Prog. Theor. Phys. **27**, 772 (1962).
[4] L. Berger, Phys. Rev. B **2**, 4559 (1970).
[5] N. Nagaosa, J. Phys. Soc. Jpn. **75**, 042001 (2006).
[6] K. A. Muttalib and P. Wölfle, Phys. Rev. B **76**, 214415 (2007).
[7] S. Onoda, N. Sugimoto, and N. Nagaosa, Phys. Rev. Lett. **97**, 126602 (2006).
[8] V. K. Dugaev, A. Crépieux, and P. Bruno, Phys. Rev. B **64**, 104411 (2001).
[9] T. Jungwirth, Q. Niu, and A. H. MacDonald, Phys. Rev. Lett. **88**, 207208 (2002).
[10] N. Nagaosa, J. Sinova, S. Onoda, A. MacDonald, and N. P. Ong, Rev. Mod. Phys. **82**, 1539 (2010).
[11] S. H. Chun, Y. S. Kim, H. K. Choi, I. T. Jeong, W. O. Lee, K. S. Suh, Y. S. Oh, K. H. Kim, Z. G. Khim, J. C. Woo, and Y. D. Park, Phys. Rev. Lett. **98**, 026601 (2007).
[12] J. Cumings, L. S. Moore, H. T. Chou, K. C. Ku, G. Xiang, S. A. Crooker, N. Samarth, and D. Goldhaber-Gordon, Phys. Rev. Lett. **96**, 196404 (2006).
[13] Y. Pu, D. Chiba, F. Matsukura, H. Ohno, and J. Shi, Phys. Rev. Lett. **101**, 117208 (2008).
[14] Y. Tian, L. Ye, and X. Jin, Phys. Rev. Lett. **103**, 087206 (2009).
[15] D. Chiba, A. Werpachowska, M. Endo, Y. Nishitani, F. Matsukura, T. Dietl, and H. Ohno, Phys. Rev. Lett. **104**, 106601 (2010).
[16] S. C. Zhang, Phys. Rev. Lett. **85**, 393 (2000).
[17] A. Richardella, P. Roushan, S. Mack, B. Zhou, D. A. Huse, D. D. Awschalom, and A. Yazdani, Science **327**, 665 (2010).
[18] P. Mitra, R. Misra, A. F. Hebard, K. A. Muttalib, and P. Wölfle, Phys. Rev. Lett. **99**, 046804 (2007).
[19] S. J. Potashnik, K. C. Ku, S. H. Chun, J. J. Berry, N. Samarth, and P. Schiffer, Appl. Phys. Lett. **79**, 1495 (2001).
[20] K. C. Ku, S. J. Potashnik, R. F. Wang, S. H. Chun, P. Schiffer, N. Samarth, M. J. Seong, A. Mascarenhas, E. Johnston-Halperin, R. C. Myers, A. C. Gossard, and D. D. Awschalom, Appl. Phys. Lett. **82**, 2302 (2003).
[21] M. J. Seong, S. H. Chun, H. M. Cheong, N. Samarth, and A. Mascarenhas, Phys. Rev. B **66**, 033202 (2002).
[22] J. Honolka, S. Masmanidis, H. X. Tang, D. D. Awschalom, and M. L. Roukes, Phys. Rev. B **75**, 245310 (2007).
[23] H. Ohno, H. Munekata, T. Penney, S. von Molnár, and L. L. Chang, Phys. Rev. Lett. **68**, 2664 (1992).
[24] B. Capoen, G. Biskupsk, and A. Briggs, J. Phys.: Condens. Matter **5**, 2545 (1993).
[25] B. L. Althsuler and A. G. Aronov, JETP Lett. **37**, 410 (1983).
[26] D. Neumaier, M. Turek, U. Wurstbauer, A. Vogl, M. Utz, W. Wegscheider, and D. Weiss, Phys. Rev. Lett. **103**, 087203 (2009).
[27] Y. Imry, J. Appl. Phys. **52**, 1817 (1981).
[28] M. C. Maliepaard, M. Pepper, R. Newbury, and G. Hill, Phys. Rev. Lett. **61**, 369 (1988).
[29] Y. Imry and Z. Ovadyahu, J. Phys. C **15**, L327 (1982).
[30] Y. Isawa, J. Phys. Soc. Jpn. **53**, 2865 (1984).
[31] M. Zhu, X. Li, G. Xiang, and N. Samarth, Phys. Rev. B **76**, 201201(R) (2007).
[32] K. Wagner, D. Neumaier, M. Reinwald, W. Wegscheider, and D. Weiss, Phys. Rev. Lett. **97**, 056803 (2006).
[33] L. Vila, R. Giraud, L. Thevenard, A. Lemaître, F. Pierre, J. Dufouleur, D. Mailly, B. Barbara, and G. Faini, Phys. Rev. Lett. **98**, 027204 (2007).
[34] C. P. Moca, B. L. Sheu, N. Samarth, P. Schiffer, B. Janko, and G. Zarand, Phys. Rev. Lett. **102**, 137203 (2009).
[35] J. G. Braden, J. S. Parker, P. Xiong, S. H. Chun, and N. Samarth, Phys. Rev. Lett. **91**, 056602 (2003).
[36] R. P. Panguluri, K. C. Ku, T. Wojtowicz, X. Liu, J. K. Furdyna, Y. B. Lyanda-Geller, N. Samarth, and B. Nadgorny, Phys. Rev. B **72**, 054510 (2005).